Published in final edited form as:

Nat Struct Mol Biol. 2011 January ; 18(1): 20–26. doi:10.1038/nsmb.1949.

Conformational changes in Dnm1 support a contractile mechanism for mitochondrial fission

Jason A. Mears[1], **Laura L. Lackner**[2], **Shunming Fang**[1], **Elena Ingerman**[2,3], **Jodi Nunnari**[2], and **Jenny E. Hinshaw**[1,¶]

[1] Laboratory of Cell Biochemistry and Biology, National Institute of Diabetes, Digestive and Kidney Diseases, National Institutes of Health, Bethesda, MD 20892

[2] Department of Molecular and Cellular Biology, Center for Genetics and Development, University of California, Davis, Davis, CA 95616

Abstract

Mitochondria are dynamic organelles that undergo cycles of fission and fusion. The yeast dynamin-related protein, Dnm1, has been localized to sites of mitochondrial division. Using cryo-electron microscopy (cryo-EM), we have determined the three-dimensional structure of Dnm1 in a GTP-bound state. The 3D map reveals a unique helical assembly for Dnm1 when compared with dynamin, a protein involved in vesicle scission during endocytosis. We also show that upon GTP hydrolysis Dnm1 constricts liposomes and subsequently dissociates from the lipid bilayer. The magnitude of Dnm1 constriction is substantially larger than the decrease in diameter previously reported for dynamin. We postulate that the larger conformational change is mediated by a flexible Dnm1 structure that has limited interaction with the underlying bilayer. Together, our structural studies support a mechanochemical role for Dnm1 during mitochondrial division.

Mitochondria regulate various cellular processes, including ATP generation, Ca^{++} maintenance, and induction of apoptosis. These tasks require dynamic mitochondria that are dependent on cycles of fission and fusion[1],[2]. Inhibition of mitochondrial division leads to an extensively interconnected and collapsed mitochondrial network within the cell as a result of unopposed fusion[2],[3]. Conversely, excessive fission or inhibition of mitochondrial fusion results in small, fragmented organelles, which are associated with aging, neurodegeneration[4], and apoptosis[5]. Conserved dynamin-related proteins (DRPs) regulate mitochondrial fission in mammals[2], plants[6] and yeast[7] and have been localized to sites of mitochondrial division[3],[8]. During mitochondrial division in yeast (Saccharomyces

Correspondence should be addressed to J.E.H. (jennyh@helix.nih.gov).

[3]Current address: Department of Cellular and Molecular Pharmacology, University of California, San Francisco, San Francisco, CA 94158

AUTHOR CONTRIBUTIONS

J.M. prepared, imaged and processed the cryo-EM data. L.L., E.I. and J.N. made the protein. S.F. processed the data. L.L. and J.N. critiqued the manuscript. J.M and J.H. analyzed the data and wrote the manuscript.

Competing interest statement The authors declare no competing financial interests.

Supplementary Information is linked to the online version of the paper at www.nature.com/nsmb/.

cerevisiae), Dnm1, a yeast DRP, is recruited to the outer mitochondrial membrane by a conserved integral membrane protein, Fis1[9], and adaptor proteins, Mdv1 and Caf4[10,11]. Both Dnm1 and Mdv1 are essential for mitochondrial fission in yeast. In mammals, Fis1[12] and the Dnm1 homolog, Drp1[2], are conserved; however, adaptor proteins homologous to Mdv1 and Caf4 have not been identified.

Proteins in the dynamin family localize to sites of membrane fission and fusion throughout the eukaryotic cell[13,14]. They contain a unique GTPase domain (Fig. 1a) that is stimulated by self-assembly through interactions with the GTPase-effector domain (GED)[15–18]. Dynamins also contain a middle domain, which also promotes self-assembly and oligomerization through interactions with the GED and through intermolecular middle domain interactions [19–24]. In addition to their conserved domain architecture (GTPase, middle and GED), dynamins contain supplementary sequences that are critical for their specific cellular functions. Dynamin, the most extensively studied family member, contains a lipid-interacting PH domain[25,26] and a proline-rich domain (PRD). The PRD contains several SH3-binding motifs that interact with additional endocytic factors [13,14]. Dnm1 lacks both the PRD and PH domain but contains an uncharacterized B-insert[2] between the middle domain and GED (Fig. 1a).

Several dynamin family members were determined to oligomerize in low salt conditions[8,20,27–29] or in the presence of nucleotide analogs[20,30–32]. For example, dynamin formed spirals in low salt[28] or in the presence of GDP/BeF[30], and Dnm1 forms spirals in the presence of non-hydrolyzable GTP analogs[20]. However, the size of the Dnm1 spirals was considerably larger than dynamin spirals, suggesting that sequence variation leads to oligomers with different dimensions. Interaction with liposomes also drives self-assembly of dynamin family members. Dynamin forms helical tubes with an outer diameter of 50 nm[33,34] that rely on PH domain interactions with negatively charged liposomes[35]. Addition of GTP to dynamin-lipid tubes leads to constriction of the tubes, followed by the dissociation of the protein from the lipid bilayer[33,36]. Dnm1 and other dynamin family members have been shown to tubulate liposomes in a similar fashion[20,21,27,32]. However, to date no GTP-induced conformational change has been observed with these protein oligomers.

The 3D structure of dynamin in the non-constricted and constricted states was solved using cryo-electron microscopy (cryo-EM) and image reconstruction methods[37,38]. The major conformational change upon GTP addition was observed in the middle/GED region[37]. Subsequent modeling studies examined the spatial arrangement of GTPase and PH domains in the constricted and non-constricted states and revealed a reorientation of GTPase domains driven by changes in the middle/GED region. These conformational changes support a model wherein a corkscrew motion within each repeating subunit of the dynamin helical array acts to mediate constriction[39].

In this manuscript, we present the first 3D structure of Dnm1-lipid tubes, solved using cryo-EM methods. When compared with dynamin, noteworthy differences are observed between the assembled molecules. Additionally, we show that Dnm1-lipid tubes constrict by ~50 nm upon addition of GTP. Unique features observed in the Dnm1 3D structure suggest how this

large conformational change is mediated. First, the helical symmetry and spacing of the Dnm1 oligomer leads to a more flexible structure. Second, no substantial interactions were observed between the protein and lipid bilayer. Dnm1 constriction reduces the underlying lipid membrane to ~20% of the starting diameter. Therefore, Dnm1 has the ability to impart a large contractile force during mitochondrial membrane fission.

RESULTS

3D reconstruction of Dnm1 helical oligomers using cryo-EM

As observed in previous studies, purified Dnm1 self-assembles into large helical assemblies when incubated with liposomes[20],[40],[41]. Here we measured the outer diameter of Dnm1-lipid tubes in the absence of nucleotide (121 ± 25 nm, n=486) and in the presence of GMP-PCP (118 ± 9 nm, n=617)(Supplementary Fig. 1). These average diameters of Dnm1-lipid tubes are consistent with the previously determined diameters of Dnm1 spirals formed *in vitro* and mitochondrial constriction sites observed *in vivo*[20]. The diameters of tubes in the presence of GMP-PCP were less variable and were therefore used to determine the 3D structure of Dnm1-lipid tubes using cryo-EM.

Before calculating a 3D volume, we first determined that the Dnm1-lipid tubes were cylindrical and not flattened using cryo-electron tomography (cryo-ET)(Fig. 1b; Supplementary Fig. 2). An orthogonal slice through the tomogram (Fig. 1b, right panel) showed that the cylindrical helices were not compressed, and therefore, were amenable for helical reconstruction methods. Next, the 3D map of Dnm1-lipid tubes was determined using the iterative helical real-space reconstruction (IHRSR) algorithm[42] to a resolution of 30 Å (see Methods). The final Dnm1 structure (Fig. 1c) has an outer diameter of 129 nm, an inner lumen of 89 nm, and 24 repeating asymmetric subunits in one turn of the helical array. When compared with previously determined cryo-EM structures of dynamin[37],[38], a similar pattern of alternating ridges and clefts are present (Fig. 1c). However, Dnm1 forms an unexpected 2-start helical structure (Fig. 1c, labeled 1 and 2; Supplementary Fig. 3a) as opposed to the single start helix of dynamin (Fig. 2a). As a result of the double helix, the Dnm1 pitch is almost 3 times larger than dynamin (28.8 nm vs. 10.6 nm, Fig. 2a), and the asymmetric unit of the Dnm1 helix is a tetramer, instead of a dimer as observed for dynamin[38] (Fig. 2b).

Dnm1 interacts weakly with the underlying lipid membrane

Another striking difference between the Dnm1 and dynamin helical structures is the interaction with the underlying lipid bilayer. Unlike dynamin, both leaflets of the lipid bilayer are clearly identifiable in the raw images of Dnm1-lipid tubes (Fig. 1, d &e) and in the final reconstruction (Fig. 1, f-i). In agreement, a 3–4 nm gap (highlighted in Fig. 2c) is observed between Dnm1 and the lipid in the 3D structure. A comparable gap was also observed in the cryo-ET reconstruction of Dnm1-lipid tubes that have not undergone averaging (Supplementary Fig. 2, e & f). Thus, the B-insert does not integrate into the lipid bilayer in a manner comparable to the PH domain of dynamin (Fig. 2c). While it is feasible that the B-insert, or another lipid-binding region, interacts directly with the lipid bilayer, this interaction must be disordered or imperceptible, as it is not seen in the averaged 3D

structure. From the raw data, it is also apparent that the gap distance between the outer leaflet of the lipid bilayer and the Dnm1 protein varies, which again suggests a weak interaction between the lipid and Dnm1.

Placement of GTPase domains within the 3D structure

To further examine the subunit organization of the helical array, the crystal structure of the GTPase domain of dynamin A from *Dictyostelium discoidum*[43] (54% identical to Dnm1) was manually fitted in the repeating asymmetric unit (Fig. 2, b & c). At the current resolution of the 3D map, we can only tentatively predict the orientation of the GTPase domains. However, the outer radial density of each asymmetric unit could easily accommodate 4 *Dicty* GTPase domain structures (Fig. 2b), and based on this fitting, 96 Dnm1 monomers occupy one helical turn (Table 1).

GTP addition leads to constriction of the Dnm1-lipid tube

Addition of 1 mM GTP to Dnm1-lipid tubes caused a significantconformational change within seconds (p-value=0.001; Fig. 3). Dnm1-lipid tubes have an average diameter of ~120 nm in the absence of nucleotide (Fig. 3, a, d & g) or under saturating amounts of a non-hydrolyzable GTP analog (1mM GMP-PCP; Fig. 3, b & e). GTP hydrolysis leads to Dnm1 constriction of the underlying lipid membrane (Fig. 3, c, f, h & i), resulting in tubes with an average outer diameter of 68 ± 22 nm (n=551) with a median score of 59 nm (Fig. 3j). The GTP-dependent changes to the Dnm1-lipid tubes were further quantified by 90° light scattering measurements. Addition of GTP to Dnm1-lipid tubes resulted in an immediate and sizable decrease in light scattering (Fig. 3k), while adding GMP-PCP had little effect. Therefore, GTP hydrolysis is required to mediate these large conformational changes, which correlates with previous findings that the Dnm1 GTPase activity is stimulated by assembly on a lipid template[40].

EM analysis also indicated that Dnm1 rapidly dissociated from the lipid following GTP-induced constriction. When Dnm1-lipid tubes were made in the absence of nucleotide, 92% of all lipid tubules were decorated with Dnm1. Five seconds after addition of GTP, we found that 69% of lipid tubes were undecorated. As shown in figure 3, several narrow (constricted) lipid tubules were devoid of protein (Fig. 3h, *), while others were less densely populated with closely associated, curved filaments of Dnm1 (Fig. 3i, arrowheads). Comparatively, dynamin remains largely associated with lipid 5 seconds after addition of GTP[36]. Lowering the GTP concentration to 0.1 mM allowed the observation of Dnm1 structural intermediates. Under these conditions, Dnm1-lipid tubes were largely decorated with protein (39% undecorated) and constricted to an average diameter of 71 ± 23 nm within 5 seconds of GTP addition (n=235, Fig. 4). After 30 seconds, a mixed population of constricted and non-constricted Dnm1-lipid tubes was observed with an average diameter of 93 ± 25 nm (n=385, Fig. 4g). The fraction of undecorated Dnm1-lipid tubes (30%) did not increase after 30 seconds, which suggests that Dnm1 can either reassemble on lipid or revert to a non-constricted state *in vitro*. Overall, these results imply that preformed Dnm1-lipid tubes undergo a large conformational change upon addition of GTP and support the model that Dnm1 can actively constrict the outer mitochondrial membrane to mediate fission *in vivo* (Fig. 5a).

Comparison of Dnm1 and Dynamin-1 helical constriction

The conformation change observed for Dnm1 is markedly larger than the constriction that has been characterized for dynamin. Upon addition of GTP, dynamin helices constrict from 50 to 40 nm[33,36]. This radial constriction is mediated by a slight ratchet motion, causing a decrease in the number of subunits per turn (14.2 to 13.2)[37], and a reorientation of dynamin domains[39], leading to a shortened radial path length (a decrease from 11.1 nm to 9.1 nm, Table 1). In contrast, the constriction observed for Dnm1 after GTP addition is considerably greater; a ~50 nm decrease in diameter. The radial path length of Dnm1 in the GTP-bound state measures 16.9 nm, so the radial spacing is 150% larger than dynamin in the non-constricted state. The radial spacing cannot be determined for Dnm1 after GTP-induced constriction because the number of subunits per turn is unknown. However, a constriction of this magnitude likely requires a substantial ratchet motion (i.e. sliding between adjacent strands). If the path length remains constant, then the number of subunits per turn would decrease by half (Table 1). Without a ratchet motion, then the radial spacing would have to decrease from 16.9 nm to 8.7 nm upon constriction, which seems unlikely. In contrast to dynamin, the driving force for Dnm1 constriction is probably a large decrease in the number of subunits per turn.

In addition to a decease in radial spacing, the distance between adjacent strands in the dynamin helix decreases (10.6 nm to 9.4 nm, Table 1; axial compression, Fig. 5b) as the structure becomes more tightly packed during constriction[37,39]. The pitch of the Dnm1 helix in the GTP-bound state was 28.8 nm, but the axial spacing between adjacent strands was 14.4 nm. As with the radial measurements, the spacing between adjacent strands of the Dnm1 helix was larger when compared with dynamin. To determine how constriction affects the axial spacing (distance between strands, Fig. 5b) of the Dnm1 array, the power spectrums of several constricted Dnm1-lipid tubes were calculated. The average distance increased from 14 nm to 21 ± 4 nm (n=28) 5 seconds after addition of 1 mM GTP and measured 18 ± 3 nm (n=26) 5 seconds after addition of 0.1 mM GTP (examples presented in Supplementary Fig. 4). Thus, Dnm1 helical constriction is associated with increased axial spacing, which could permit sliding of adjacent strands needed to mediate the large decrease in tube diameter.

DISCUSSION

Here we present the 3D structure of Dnm1 helical tubes and reveal a large conformational change that generates a contractile force on lipid bilayers. The magnitude of constriction is large enough to resolve how a ~120 nm Dnm1 helical array can facilitate the fission of the outer mitochondrial membrane. Furthermore, Dnm1-lipid tubes were observed over a wide range of diameters in different nucleotide states (121 ± 25 nm in the absence of nucleotide and 118 ±v9 nm in the presence of GMP-PCP). These variations suggest that the Dnm1 oligomer has an inherent plasticity that allows it to generate helical structures with a wide range of diameters. This is in contrast to dynamin-lipid tubes, where the diameter is less diverse (52 ± 4 nm)[33]. The diameters of the necks of budding vesicles, where dynamin is targeted, are more defined, and a host of cofactors may shape this structure before dynamin binds[44–46]. The structural variability of Dnm1 may be an essential feature that is required to

accommodate the heterogeneity of mitochondrial sizes *in vivo*. Additionally, this helical plasticity may play a fundamental role in the constriction event. The Dnm1 oligomer must undergo large domain reorientations during constriction to allow for the considerable bending of the Dnm1 filament (i.e. the strand of the helical array). The final 3D structure of the Dnm1 helix demonstrates two key features that could facilitate the observed constriction: the helical structure is more loosely packed than comparable structures of dynamin (Table 1), and the protein is not anchored in the underlying lipid bilayer (Fig. 2c).

Sequence comparison of Dnm1 with dynamin suggests that the mechanochemical core (i.e. GTPase, middle and GED regions) of Dnm1 is preserved. As with dynamin, a GTP-dependent conformational change may reorient the protein domains to trigger a ratchet motion, but the magnitude of the constriction would be much larger for Dnm1. Recent x-ray structures of a dynamin GTPase-GED fusion protein[15] and the middle-GED regions of dynamin-like MxA[19] provide clues to the mechanisms of oligomerization and assembly-stimulated GTPase activity. Amino acids in both the GTP-binding pocket and GTPase-GED bundle are conserved in Dnm1, which suggests that these residues are crucial for dynamin and Dnm1. The dimer structure of the dynamin GTPase-GED fusion protein represents a transition state, and the dimer interface was not observed in the GTP bound state. Therefore, our Dnm1 structure in the GTP-bound state represents a different conformation that precedes hydrolysis. Because the domain architectures of Dnm1 and dynamin are similar, the middle and GED domains from Dnm1 are predicted to fit in the middle radial density at the cleft (highlighted in Fig. 2b). The Dnm1 middle domain-GED helices are likely similar to the structures observed in the MxA stalk structure[19]. However, the relative orientation between adjacent subunits may be different due to the larger radius of curvature and radial spacing in the Dnm1 structure. The B-insert could also fit in this area, which may affect the intra- and intermolecular interactions between the middle domain and GED and increase the size of this radial density. Noticeably, the strongest feature of the 3D map is the middle radial density.

GTPase domain interactions observed in the dynamin structure[15] are predicted to occur between sequential turns of the dynamin helix[19]. Because the Dnm1 structure is a 2-start helix, GTPase domain interactions are between the two strands of the helix. GTP binding leads to a decrease in the variability in diameters of Dnm1-lipid tubes, which is consistent with an enhanced stability provided by interactions between adjacent GTPase domains. GTP hydrolysis may trigger conformational changes in the GTPase domains that destabilize lateral (or axial) interactions in the helix. The larger distances observed between the ridges of the Dnm1 helix would allow for sliding of adjacent strands (Figs. 2a & 5b) and thereby permit large ratchet motions needed to constrict the underlying membrane to a diameter that begins to approach the size needed for fission. This large sliding motion would require strong radial interactions, facilitated by the middle-GED assembly, to preserve the Dnm1 filament in each turn of the helix. In agreement, the middle radial density in the Dnm1 structure is the strongest feature of the map, and a mutation in the middle domain abolishes filament formation[20]. Moreover, we observed large Dnm1 filaments dissociating from the lipid upon GTP hydrolysis (inset panels, Fig. 3i), which is consistent with the idea that strands of Dnm1 remain intact during constriction. The large distribution of diameters for

Dnm1-lipid tubes after addition of GTP (Figs. 3j and 4, f & g) also demonstrates that several filament curvatures exist during intermediate states of constriction.

Dnm1 lacks a predicted lipid-binding domain. In place of a PH domain[25],[35], Dnm1 contains an uncharacterized B-insert (Fig 1a) that is disordered based on secondary structure analyses. Although we cannot resolve the position of the B-insert in our 3D structure, our results suggest that Dnm1 is not strongly anchored in the outer leaflet of the lipid bilayer (Fig. 2c). Because the Dnm1 middle radial density is appreciably larger than dynamin, it is possible that the B-insert is contained within the middle radial density and affects the interactions between the middle domain and GED. Therefore, the large diameter of the Dnm1-lipid tubes could be related to the presence of the B-insert in the self-assembly region (middle/GED) of the Dnm1 oligomer. The B-insert could also contain a flexible loop between the middle domain and GED and may have an affinity for lipids that reflect non-specific electrostatic interactions. Regardless, the lipid bilayer acts to nucleate Dnm1 oligomers that grow into larger helical structures *in vitro*. Consistent with this idea, we find that the Dnm1 helices often extend beyond underlying lipid tubules. Thus, conformational changes in Dnm1 are not dictated by lipid restraints, and the protein can glide over the lipid bilayer during helical constriction (Fig. 5b).

The distance necessary for spontaneous membrane fission between juxtaposed leaflets of a lipid bilayer has been calculated to be 1–2 nm[47],[48]. At first, it appears that the average luminal diameter of Dnm1 lipid-tubes in the constricted state (averaging ~20 nm, Table 1) is not sufficient to complete the fission process. However, mitochondria are comprised of a double membrane, and, consequently, the lumen of the inner mitochondrial membrane could approach the required diameter for fission upon Dnm1-mediated constriction of the outer membrane. Furthermore, a considerable number (~15%) of Dnm1-lipid tubes observed had outer radial diameters approaching 40 nm upon addition of GTP. This size is comparable to the diameter of dynamin in the constricted state, and recent studies have shown that dynamin alone can mediate membrane fission[47],[49],[50]. Thus, a small subset of Dnm1 constriction events observed *in vitro* exhibits luminal diameters approaching the distance needed for fission (consistently <10 nm). Moreover, Dnm1 could undergo multiple rounds of constriction, and only when the inner lumen approaches a diameter of less than 10 nm does the lipid resist additional constriction.

In vivo, additional factors and forces likely regulate and facilitate this membrane fission event. For example, after targeting Dnm1 to membranes, Mdv1 nucleates Dnm1 assembly on the lipid surface[40]. This interaction with Mdv1 may tether Dnm1 to the outer mitochondrial membrane allowing for multiple rounds of constriction *in vivo*, and thereby enhance the contractile force of Dnm1 during mitochondrial division. Consistent with this role for adaptors, the 3–4 nm gap between Dnm1 and the lipid membrane in our 3D map could easily accommodate protein cofactors required for mitochondrial fission. For dynamin, the PH domain is found at the interface between the lipid and the conserved core of dynamin and anchors the protein in the bilayer during constriction. In place of the PH domain, the cytoplasmic domain of Fis1[51], or the WD repeat domain[52] within Mdv1 and Caf4 that interacts with Dnm1, could fit in the gap between Dnm1 and the lipid bilayer, and thereby anchor Dnm1 near the lipid during constriction. In the future, *in vitro* studies of

Dnm1 and these partners will address their roles in regulating the structure of the mitochondrial fission machinery.

In conclusion, our results provide new insight into the mechanism of mitochondrial fission and support an active role for Dnm1 in the constriction of mitochondrial membrane(s). This model is broadly applicable given the conservation of dynamin-related proteins involved in mitochondrial fission throughout all eukaryotes. Furthermore, Dnm1 is required for peroxisomal fission, which suggests that a similar mechanism likely mediates this process. Dnm1 constriction also provides evidence that a common mechanism exists for dynamin family members involved in membrane fission. Both dynamin and now Dnm1 have been shown to actively constrict the underlying lipid bilayer upon GTP hydrolysis, and the magnitude of constriction for both is ideally suited for their distinct cellular functions.

METHODS

Protein expression and purification

Dnm1 was expressed and purified as described previously[20]. In brief, high titer virus containing the Dnm1 expression plasmid was used to infect Hi5 insect cells for protein expression. Infected cells were collected after 48 h of infection and were stored at −80°C. Infected cells were thawed at RT and resuspended in wash buffer (25 mM Hepes, 25 mM Pipes, pH 7.0, 500 mM NaCl, and 80 mM imidazole, pH 7.4) containing protease inhibitor cocktail 1 (Calbiochem). Resuspended thawed cells were lysed and the lysate was centrifuged at 60,000*g* for 30 min. Dnm1 was purified from the supernatant using a HiTrap metal chelating column attached to an AKTA prime system (GE Healthcare). Dnm1 was eluted from the column by using a linear gradient of 25 mM Hepes, 25 mM Pipes, pH 7.0, 500 mM NaCl, and 500 mM imidazole, pH 7.4. DMSO was added to purified Dnm1 to a final concentration of 20%, rendering the freezing buffer 20 mM Hepes, 20 mM Pipes, 400 mM imidazole, and 20% v/v DMSO. Purified protein was frozen in liquid nitrogen and stored at −80°C.

Dnm1-lipid tube formation

To begin, a 50 μl mixture of phosphatidylethanolamine (0.45 mg) and phosphatidylinositol 4-phosphate (0.05mg) in chloroform (Avanti Polar Lipids) was dried under nitrogen gas. 100% v/v phosphatidylserine (PS) was used on occasion with no difference in results. Dried lipid was resuspended in HCB150 buffer (20 mM Hepes, pH 7.2, 1 mM $MgCl_2$, 2 mM EGTA and 150 mM NaCl) to a final concentration of 2 mg ml^{-1}. To make Dnm1-lipid tubes, the protein was diluted (~0.1 mg ml^{-1}, 1.2 μM) in HCB150 and resuspended lipid was then added to a final concentration of 0.1–0.2 mg ml^{-1} and incubated at room temperature for 2 hrs. For samples with nucleotide, GTP or GMP-PCP (Sigma) was added to a final concentration of either 0.1 or 1.0 mM. P-values were calculated by one-way ANOVA (GraphPad Prism 5).

EM sample praparation

For negative stain, samples were stained with 2% w/v uranyl acetate (EM Sciences) on carbon-coated grids. For cryo-EM preparations, samples were applied to holey carbon grids

(R3.5/1, Quantifoil), blotted and frozen in liquid ethane using a Vitrobot (FEI Co.) system. Negative stain and cryo-EM images not used for high-resolution reconstructions were recorded on a CM120 (Philips) microscope operating at 100 kV using a Gatan 1k x 1k CCD camera.

Cryo-ET reconstruction

A single-axis tilt series was collected on a Tecnai-12 electron microscope (FEI) operating at 120 keV. The microscope was equipped with an energy filter (Gatan GIF 2002) that was operated in the zero-energy-loss mode with a slit width of 20 eV. Images were recorded on a 2,048 × 2,048-pixel CCD camera (Gatan) at ×45,000 magnification (0.67-nm pixels) and 4–6 μm defocus. Data were recorded at 1° steps, covering ranges of approximately −56° to +56° under low-dose conditions, using SerialEMsoftware[53] to conduct automatic tilting, tracking, focusing, and image acquisition. Projections were aligned without fiducial markers and the tomogram was calculated using IMOD[54].

3D reconstruction and representation

High-resolution cryo-EM images were recorded at 50,000 X magnification using film (Kodak SO163) on a CM200 FEG (Philips) microscope operating at 120 kV. Films were digitized using a Leafscan 45 scanner at a step size of 12.5 μm, and the images were binned twice to 5 Å/pixel. Selected Dnm1-lipid tubes with good diffraction and minimum astigmatism and drift were initially boxed into helical segments using the helixboxer and boxer programs in the EMAN suite[55]. The segments used in the final reconstruction were 300 X 300 pixels. Projection matching was used to sort 4,323 boxed segments based on tube diameter. The average diameter for the complete dataset was comparable to the values shown in Supplementary Figure 1. It was determined that the helical segments with diameters approaching 130 nm were most homogeneous. 600 manually screened segments were used for final refinement. During each of the 50 iterative cycles of the IHRSR[42] refinement, a 3° limit was used for in-plane tilt correction and a cross-correlation threshold was used to ensure a homogeneous dataset. 430 images with ~125 asymmetric subunits in each boxed segment were used in the final reconstruction, corresponding to 53,750 repeating subunits. The final reconstruction resolved to a 2-start structure with 24.0 subunits per turn and a helical pitch of 288 Å (Fig. 1c and Supplementary Fig. 3e). The resolution was determined to be ~30 Å (0.5 FSC criterion). Chimera[56] was used for representation of the 3D volumes and to manually fit dyn A GTPase domains (PDB ID: 1JWY, chain B) into the Dnm1 structure. See Supplementary Methods for more detail.

Tube morphology and decoration

Tube diameters and the amount of Dnm1 decoration on lipid tubules were measured using the ImageJ software (available at http://rsb.info.nih.gov/ij). The amount of protein decoration was measured per length of all lipid tubules (i.e. protein decoration on liposomes was not counted). The total distances measured were 16.6 μm for tubes formed in the absence of nucleotide, 16.4 μm for tubes treated with 1 mM GTP for 5 s, and 5.7 μm and 8.3 μm for tubes treated with 0.1 mM GTP for 5s and 30s, respectively.

90° light scattering

Dnm1-lipid tubes were diluted 1:4 with HCB150 to a final concentration of ~25 μg ml^{-1} (0.3 μM). A Photon Technology International (PTI) Model 814 photomultiplier was used at 350 nm excitation and 355 nm emission with excitation and emission slit widths set at 3 mm. Measurements were collected at 0.1 s intervals. After obtaining a stable background, GTP (1 mM final) was added to Dnm1 samples. Data was collected and analyzed using the Felix 32 software (PTI).

Supplementary Material

Refer to Web version on PubMed Central for supplementary material.

Acknowledgments

We thank D. Winkler and A. Steven for technical assistance in acquiring tomograms; P. Flicker, J. Hanover, W. Prinz, J. Evans, and J. Heymann for critical discussions and reading of the manuscript. This work was supported by the Intramural Research Program of the NIH, NIDDK (J.E.H.) and the Nancy Nossal Fellowship of the NIH, NIDDK (J.A.M.), J.N. is supported by NIH grant R01GM062942, and L.L.L. is supported by NIH postdoctoral fellowship 1F32GM078749.

References

1. Hoppins S, Lackner L, Nunnari J. The machines that divide and fuse mitochondria. Annu Rev Biochem. 2007; 76:751–780. [PubMed: 17362197]
2. Smirnova E, Shurland DL, Ryazantsev SN, van der Bliek AM. A human dynamin-related protein controls the distribution of mitochondria. J Cell Biol. 1998; 143:351–358. [PubMed: 9786947]
3. Bleazard W, et al. The dynamin-related GTPase Dnm1 regulates mitochondrial fission in yeast. Nat Cell Biol. 1999; 1:298–304. [PubMed: 10559943]
4. Knott AB, Perkins G, Schwarzenbacher R, Bossy-Wetzel E. Mitochondrial fragmentation in neurodegeneration. Nat Rev Neurosci. 2008; 9:505–518. [PubMed: 18568013]
5. Frank S, et al. The role of dynamin-related protein 1, a mediator of mitochondrial fission, in apoptosis. Dev Cell. 2001; 1:515–525. [PubMed: 11703942]
6. Arimura S, Tsutsumi N. A dynamin-like protein (ADL2b), rather than FtsZ, is involved in Arabidopsis mitochondrial division. Proc Natl Acad Sci U S A. 2002; 99:5727–5731. [PubMed: 11960028]
7. Otsuga D, et al. The dynamin-related GTPase, Dnm1p, controls mitochondrial morphology in yeast. J Cell Biol. 1998; 143:333–349. [PubMed: 9786946]
8. Smirnova E, Griparic L, Shurland DL, van der Bliek AM. Dynamin-related protein Drp1 is required for mitochondrial division in mammalian cells. Mol Biol Cell. 2001; 12:2245–2256. [PubMed: 11514614]
9. Mozdy AD, McCaffery JM, Shaw JM. Dnm1p GTPase-mediated mitochondrial fission is a multi-step process requiring the novel integral membrane component Fis1p. J Cell Biol. 2000; 151:367–380. [PubMed: 11038183]
10. Griffin EE, Graumann J, Chan DC. The WD40 protein Caf4p is a component of the mitochondrial fission machinery and recruits Dnm1p to mitochondria. J Cell Biol. 2005; 170:237–248. [PubMed: 16009724]
11. Tieu Q, Okreglak V, Naylor K, Nunnari J. The WD repeat protein, Mdv1p, functions as a molecular adaptor by interacting with Dnm1p and Fis1p during mitochondrial fission. J Cell Biol. 2002; 158:445–452. [PubMed: 12163467]
12. James DI, Parone PA, Mattenberger Y, Martinou JC. hFis1, a novel component of the mammalian mitochondrial fission machinery. J Biol Chem. 2003; 278:36373–36379. [PubMed: 12783892]

13. Heymann JA, Hinshaw JE. Dynamins at a glance. J Cell Sci. 2009; 122:3427–3431. [PubMed: 19759282]
14. Praefcke GJ, McMahon HT. The dynamin superfamily: universal membrane tubulation and fission molecules? Nat Rev Mol Cell Biol. 2004; 5:133–147. [PubMed: 15040446]
15. Chappie JS, Acharya S, Leonard M, Schmid SL, Dyda F. G domain dimerization controls dynamin's assembly-stimulated GTPase activity. Nature. 2010
16. Chappie JS, et al. An intramolecular signaling element that modulates dynamin function in vitro and in vivo. Mol Biol Cell. 2009; 20:3561–3571. [PubMed: 19515832]
17. Muhlberg AB, Warnock DE, Schmid SL. Domain structure and intramolecular regulation of dynamin GTPase. EMBO J. 1997; 16:6676–6683. [PubMed: 9362482]
18. Song BD, Yarar D, Schmid SL. An assembly-incompetent mutant establishes a requirement for dynamin self-assembly in clathrin-mediated endocytosis in vivo. Mol Biol Cell. 2004; 15:2243–2252. [PubMed: 15004222]
19. Gao S, et al. Structural basis of oligomerization in the stalk region of dynamin-like MxA. Nature. 2010
20. Ingerman E, et al. Dnm1 forms spirals that are structurally tailored to fit mitochondria. J Cell Biol. 2005; 170:1021–1027. [PubMed: 16186251]
21. Low HH, Sachse C, Amos LA, Lowe J. Structure of a bacterial dynamin-like protein lipid tube provides a mechanism for assembly and membrane curving. Cell. 2009; 139:1342–1352. [PubMed: 20064379]
22. Okamoto PM, Tripet B, Litowski J, Hodges RS, Vallee RB. Multiple distinct coiled-coils are involved in dynamin self-assembly. J Biol Chem. 1999; 274:10277–10286. [PubMed: 10187814]
23. Ramachandran R, et al. The dynamin middle domain is critical for tetramerization and higher-order self-assembly. EMBO J. 2007; 26:559–566. [PubMed: 17170701]
24. Smirnova E, Shurland DL, Newman-Smith ED, Pishvaee B, van der Bliek AM. A model for dynamin self-assembly based on binding between three different protein domains. J Biol Chem. 1999; 274:14942–14947. [PubMed: 10329695]
25. Klein DE, Lee A, Frank DW, Marks MS, Lemmon MA. The pleckstrin homology domains of dynamin isoforms require oligomerization for high affinity phosphoinositide binding. J Biol Chem. 1998; 273:27725–27733. [PubMed: 9765310]
26. Zheng J, et al. Identification of the binding site for acidic phospholipids on the pH domain of dynamin: implications for stimulation of GTPase activity. J Mol Biol. 1996; 255:14–21. [PubMed: 8568861]
27. Accola MA, Huang B, Al Masri A, McNiven MA. The antiviral dynamin family member, MxA, tubulates lipids and localizes to the smooth endoplasmic reticulum. J Biol Chem. 2002; 277:21829–21835. [PubMed: 11916975]
28. Hinshaw JE, Schmid SL. Dynamin self-assembles into rings suggesting a mechanism for coated vesicle budding. Nature. 1995; 374:190–192. [PubMed: 7877694]
29. Kim YW, et al. Arabidopsis dynamin-like 2 that binds specifically to phosphatidylinositol 4-phosphate assembles into a high-molecular weight complex in vivo and in vitro. Plant Physiol. 2001; 127:1243–1255. [PubMed: 11706203]
30. Carr JF, Hinshaw JE. Dynamin assembles into spirals under physiological salt conditions upon the addition of GDP and gamma-phosphate analogues. J Biol Chem. 1997; 272:28030–28035. [PubMed: 9346955]
31. Kochs G, Haener M, Aebi U, Haller O. Self-assembly of human MxA GTPase into highly ordered dynamin-like oligomers. J Biol Chem. 2002; 277:14172– 14176. [PubMed: 11847228]
32. Yoon Y, Pitts KR, McNiven MA. Mammalian dynamin-like protein DLP1 tubulates membranes. Mol Biol Cell. 2001; 12:2894–2905. [PubMed: 11553726]
33. Sweitzer SM, Hinshaw JE. Dynamin undergoes a GTP-dependent conformational change causing vesiculation. Cell. 1998; 93:1021–1029. [PubMed: 9635431]
34. Takei K, Slepnev VI, Haucke V, De Camilli P. Functional partnership between amphiphysin and dynamin in clathrin-mediated endocytosis. Nat Cell Biol. 1999; 1:33–39. [PubMed: 10559861]

35. Vallis Y, Wigge P, Marks B, Evans PR, McMahon HT. Importance of the pleckstrin homology domain of dynamin in clathrin-mediated endocytosis. Curr Biol. 1999; 9:257–260. [PubMed: 10074456]
36. Danino D, Moon KH, Hinshaw JE. Rapid constriction of lipid bilayers by the mechanochemical enzyme dynamin. J Struct Biol. 2004; 147:259–267. [PubMed: 15450295]
37. Chen YJ, Zhang P, Egelman EH, Hinshaw JE. The stalk region of dynamin drives the constriction of dynamin tubes. Nat Struct Mol Biol. 2004; 11:574–575. [PubMed: 15133500]
38. Zhang P, Hinshaw JE. Three-dimensional reconstruction of dynamin in the constricted state. Nat Cell Biol. 2001; 3:922–926. [PubMed: 11584275]
39. Mears JA, Ray P, Hinshaw JE. A corkscrew model for dynamin constriction. Structure. 2007; 15:1190–1202. [PubMed: 17937909]
40. Lackner LL, Horner JS, Nunnari J. Mechanistic analysis of a dynamin effector. Science. 2009; 325:874–877. [PubMed: 19679814]
41. Mears JA, Hinshaw JE. Visualization of dynamins. Methods Cell Biol. 2008; 88:237–256. [PubMed: 18617037]
42. Egelman EH. A robust algorithm for the reconstruction of helical filaments using single-particle methods. Ultramicroscopy. 2000; 85:225–234. [PubMed: 11125866]
43. Niemann HH, Knetsch ML, Scherer A, Manstein DJ, Kull FJ. Crystal structure of a dynamin GTPase domain in both nucleotide-free and GDP-bound forms. EMBO J. 2001; 20:5813–5821. [PubMed: 11689422]
44. Doherty GJ, McMahon HT. Mechanisms of endocytosis. Annu Rev Biochem. 2009; 78:857–902. [PubMed: 19317650]
45. Ferguson S, et al. Coordinated actions of actin and BAR proteins upstream of dynamin at endocytic clathrin-coated pits. Dev Cell. 2009; 17:811–822. [PubMed: 20059951]
46. Roux A, et al. Membrane curvature controls dynamin polymerization. Proc Natl Acad Sci U S A. 2010; 107:4141–4146. [PubMed: 20160074]
47. Bashkirov PV, et al. GTPase cycle of dynamin is coupled to membrane squeeze and release, leading to spontaneous fission. Cell. 2008; 135:1276–1286. [PubMed: 19084269]
48. Kozlovsky Y, Kozlov MM. Membrane fission: model for intermediate structures. Biophys J. 2003; 85:85–96. [PubMed: 12829467]
49. Pucadyil TJ, Schmid SL. Real-time visualization of dynamin-catalyzed membrane fission and vesicle release. Cell. 2008; 135:1263–1275. [PubMed: 19084268]
50. Roux A, Uyhazi K, Frost A, De Camilli P. GTP-dependent twisting of dynamin implicates constriction and tension in membrane fission. Nature. 2006; 441:528–531. [PubMed: 16648839]
51. Zhang Y, Chan DC. Structural basis for recruitment of mitochondrial fission complexes by Fis1. Proc Natl Acad Sci U S A. 2007; 104:18526–18530. [PubMed: 17998537]
52. Johnston CA, Kimple AJ, Giguere PM, Siderovski DP. Structure of the parathyroid hormone receptor C terminus bound to the G-protein dimer Gbeta1gamma2. Structure. 2008; 16:1086–1094. [PubMed: 18611381]
53. Mastronarde DN. Automated electron microscope tomography using robust prediction of specimen movements. J Struct Biol. 2005; 152:36–51. [PubMed: 16182563]
54. Kremer JR, Mastronarde DN, McIntosh JR. Computer visualization of three-dimensional image data using IMOD. J Struct Biol. 1996; 116:71–76. [PubMed: 8742726]
55. Ludtke SJ, Baldwin PR, Chiu W. EMAN: semiautomated software for high- resolution single-particle reconstructions. J Struct Biol. 1999; 128:82–97. [PubMed: 10600563]
56. Pettersen EF, et al. UCSF Chimera--a visualization system for exploratory research and analysis. J Comput Chem. 2004; 25:1605–1612. [PubMed: 15264254]

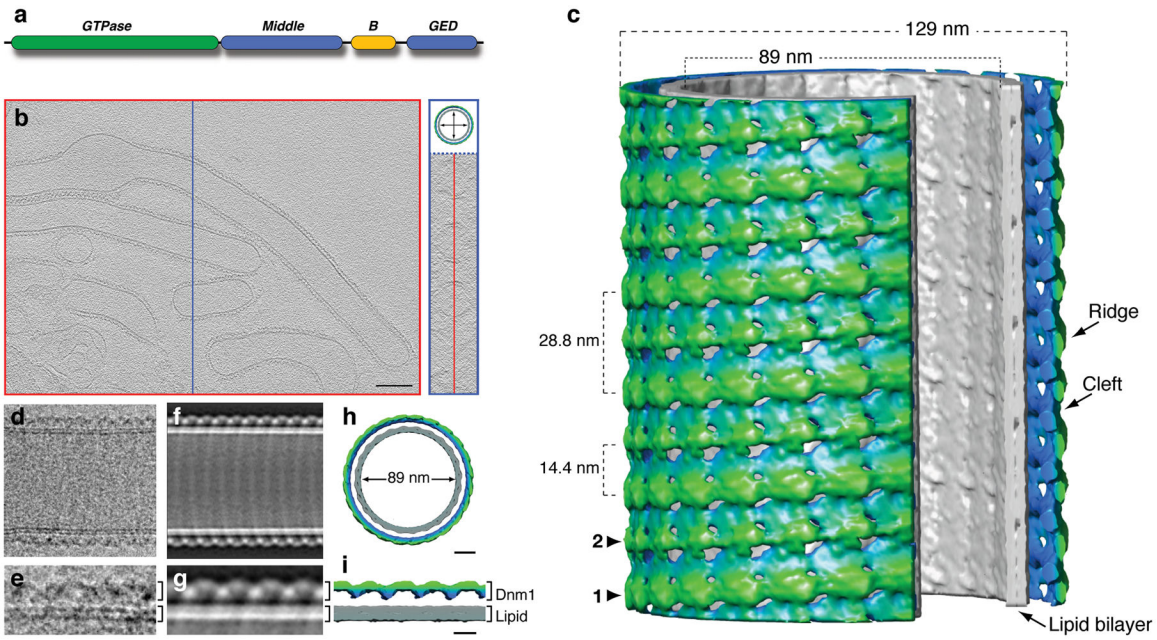

Figure 1.

3D reconstructions of Dnm1 helices. **(a**) The primary sequence of Dnm1 contains 4 domains: GTPase, middle, B-insert and GTPase-effector (GED). **(b)** A cryo-ET reconstruction of Dnm1-lipid tubes is shown from two orthogonal perspectives. The cylindrical shape of the helices is highlighted adjacent to a central z-slice by an end view of the tomogram of Dnm1 (blue box). Scale bar, 100 nm. (**c**) The 3D structure of the Dnm1 tube is presented with a wedge of the helix removed to show a representative cross-section. The protein is colored with a radial gradient (blue near the lipid to green at the periphery). The lipid bilayer is grey. The outer diameter (129 nm), inner lumen (89 nm), helical pitch (28.8 nm), the two helical starts (labeled 1 and 2) and the spacing between each start (14.4 nm) are highlighted. The lipid bilayer, ridge and cleft features are indicated. (**d)** A representative raw image of the Dnm1 tubes. (**e)** One side of the raw image highlights the gap between lipid and protein. (**f)** An average 2D projection of the final Dnm1 reconstruction. (**g)** One side of the 2D projection. (**h)**, End view of the final 3D structure. Scale bar, 20 nm. **(i)** A cross-section of the final 3D map highlights the gap between Dnm1 and the lipid bilayer (compare with **e** & **g)**. Scale bar, 10 nm.

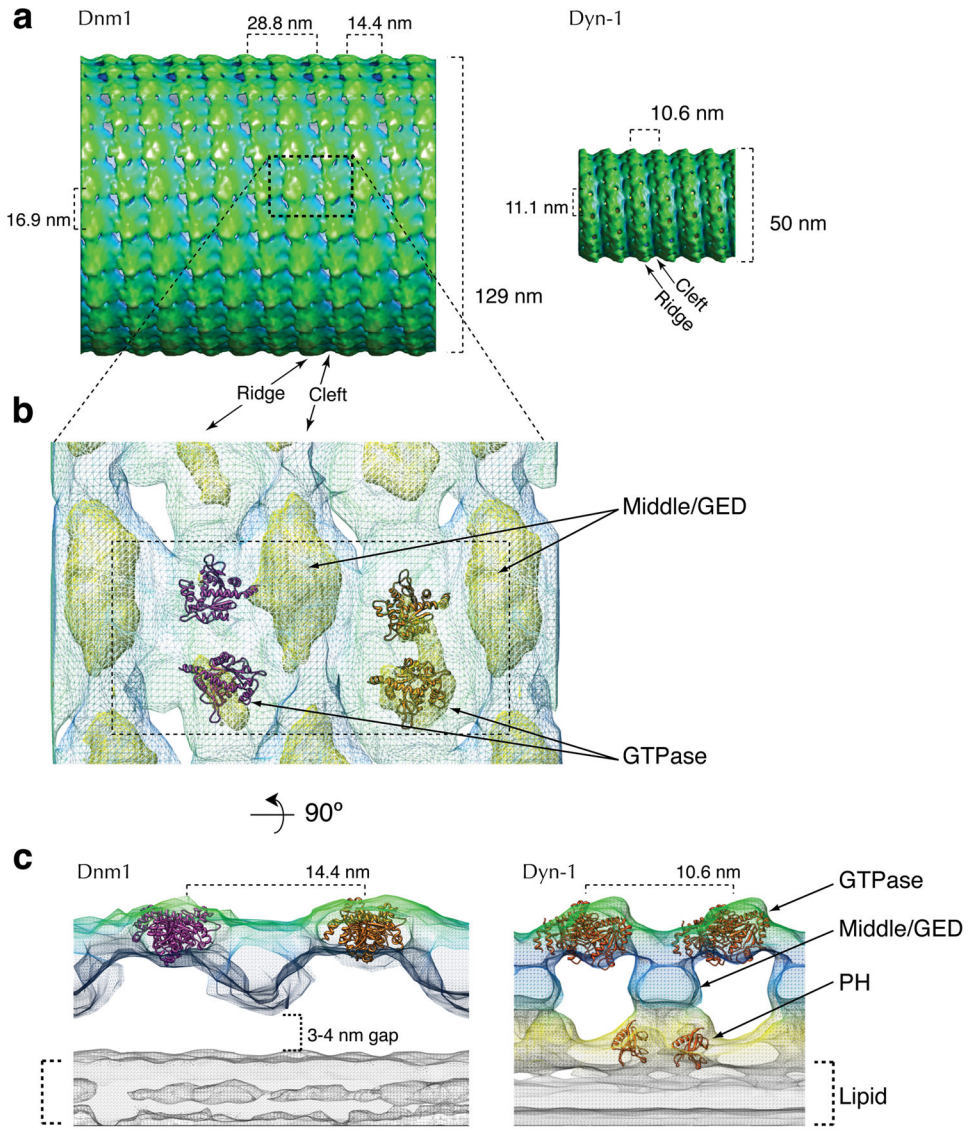

Figure 2.

An analysis of Dnm1 helical packing. **(a)** Comparison between Dnm1 and ΔPRD-dynamin 1 (Dyn-1) structures[37]. The helical pitch is 28.8 nm for Dnm1 and 10.6 nm for dynamin. The axial spacing between the two starts of the Dnm1 helix is 14.4 nm. The outer diameters (129 nm and 50 nm, respectively), radial path lengths (16.9 nm and 11.1 nm, respectively), ridge and cleft features are also indicated. The outer radial density (green) and the inner radial density (blue) are where the GTPase domains and the middle/GED domains are predicted to reside, respectively. (**b**) Four GTPase domain crystal structures from dyn A (PDB ID: 1JX2, chain B) were manually fitted to one asymmetric subunit of the Dnm1 helical structure. Two dimers found in separate helical starts of the asymmetric subunit are colored purple and orange, respectively. Two density thresholds are presented (low threshold, blue-green; high threshold, yellow). The dashed box highlights the region presented in **c** (left panel) after a 90° rotation. (**c**) Fittings of GTPase domains are compared between Dnm1 (left) and

Dyn-1[39] (right). A 3–4 nm gap between Dnm1 and the lipid bilayer (grey) exists where the PH domain (orange ribbon, yellow mesh) of Dyn-1 resides.

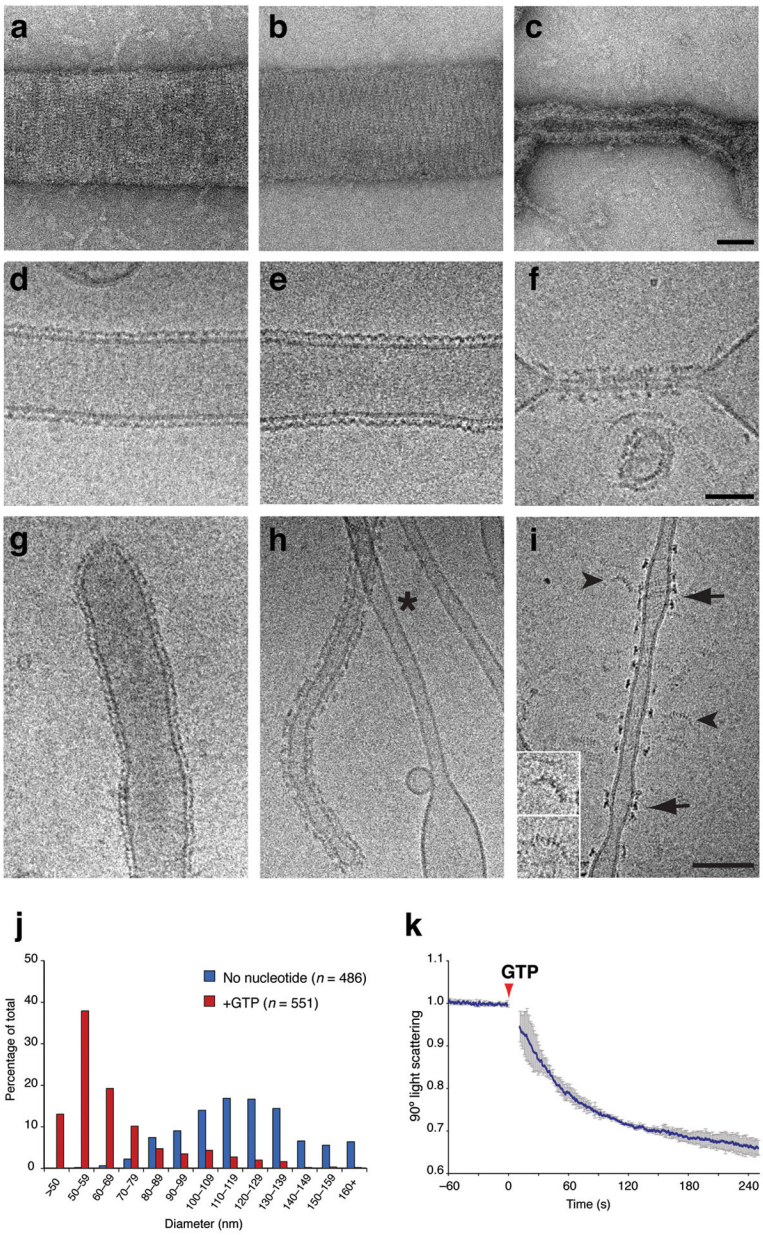

Figure 3.

Dnm1-lipid tubes constrict upon addition of GTP. (**a**–**i**) Dnm1-lipid tubes were imaged using negative stain EM (**a**–**c**) and cryo-EM (**d**–**i**). Dnm1 tubes in the absence of nucleotide (**a, d** & **g**), in the presence of GMP-PCP (**b** & **e**), and after addition of 1 mM GTP (**c**, **f**, **h** & **i**). Scale bars, 50 nm (**a**–**f**) and 100 nm (**g**–**i**). Bare lipid tubes (**h**, *), regions where Dnm1 filaments are loosely packed (**i**, arrows), and Dnm1 filaments that have dissociated from the membrane (**i**, arrowheads and insets) are highlighted. (**j**) Distributions of tube diameters for Dnm1 tubes treated with or without 1 mM GTP for 5 seconds. (**k**) 90° light scattering of Dnm1 tubes decreased upon addition of 1 mM GTP (red arrow).

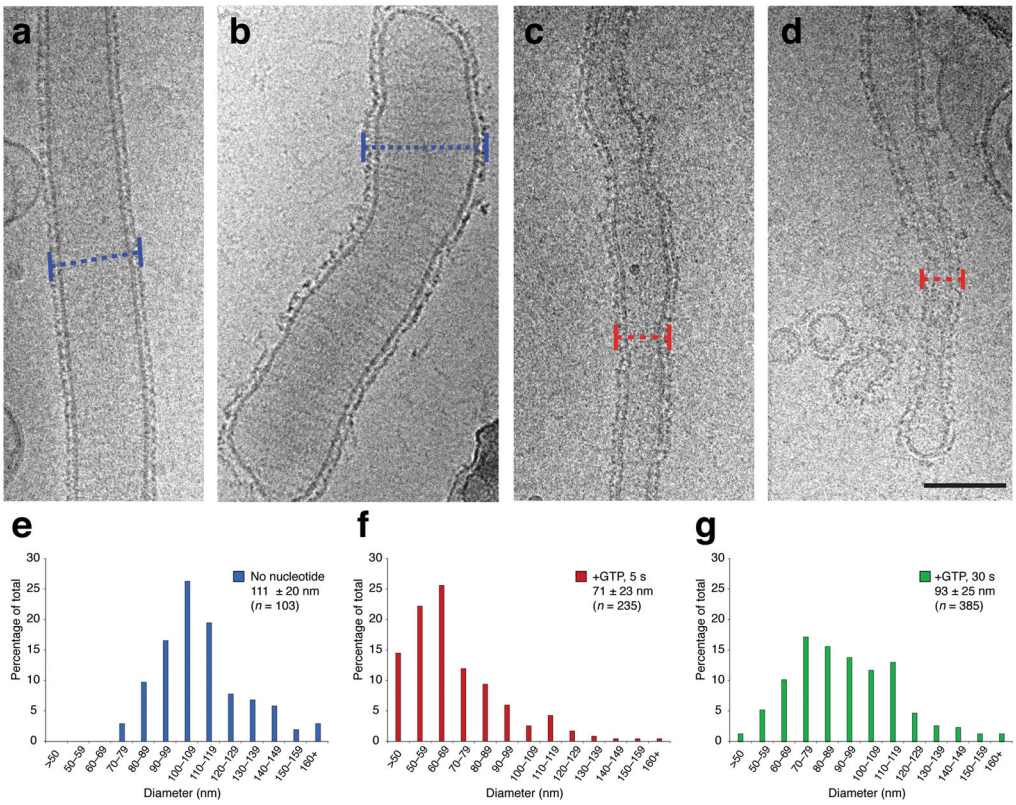

Figure 4.

The diameters of Dnm1-lipid tubes recover after an initial constriction. **(a–d)** Cryo-EM images of Dnm1-lipid tubes in the absence of GTP (**a** & **b**) and 5 seconds after addition of 0.1 mM GTP (**c** & **d**). Scale bar, 100 nm. (**e–g**) Distribution of Dnm1 tube diameters before (**e**) and after (**f**, 5 sec and **g**, 30 sec) addition of 0.1 mM GTP were measured. Corresponding outer tube diameters are highlighted by dashed blue lines (no GTP) in panels **a** (110 nm) and **b** (150 nm) and by dashed red lines (0.1 mM GTP, 5 sec) in **c** (65 nm) and **d** (50 nm).

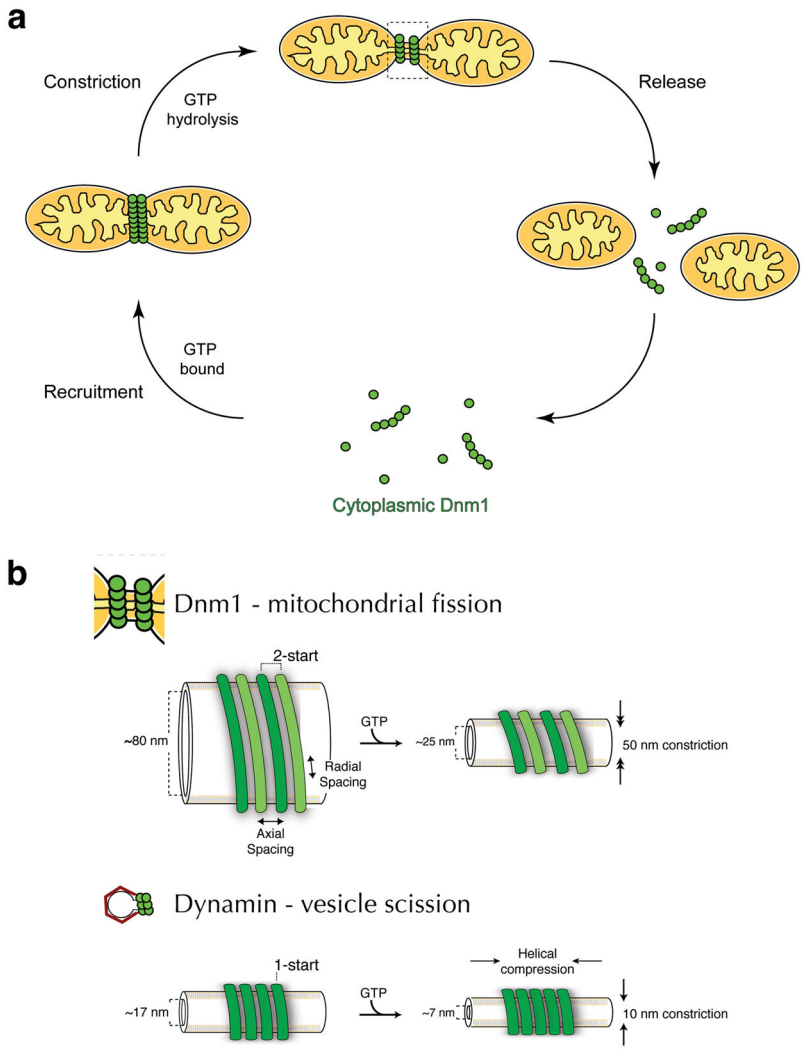

Figure 5.

A model for mitochondrial fission. **(a)** An active contractile force is proposed to play a role in mitochondrial fission, where Dnm1 is recruited to mitochondria and constricts the underlying membrane(s), which leads to fission and release of the protein. (**b**) Differences in helical packing and GTP-induced conformational changes between Dnm1 and Dyn-1 are compared. Unlike Dyn-1, Dnm1 assembles as a two-start helix and no axial compression is observed upon addition of GTP. The inner lumen of Dnm1 tubes decrease from ~80 nm to ~25 nm, while dynamin decreases from ~20 nm to ~10 nm.

Table 1

Comparison of Dnm1 and Dynamin helical properties

	Dnm1 (Non-constricted)	Dnm1 (Constricted)	ΔPRD-Dynamin[1] (Non-constricted)	ΔPRD-Dynamin[1] (Constricted)
Outer Diameter (nm)	129	67 (59)[3]	50	40
Lumen Diameter (nm)	89	25 (19)[3]	17	7
Helical pitch (nm)	28.8	ε 28.8[4]	10.6	9.4
# subunits per turn (n)	24.0	12.4[5]	14.2	13.2
Monomers per turn	96 (48)[2]	50 (25)[6]	28	26
Circumference (C=πD, nm)	405	210	157	126
Path length (p=C/n, nm)	16.9	16.9[5]	11.1	9.1

[1] Values taken from Chen et al. (2004)

[2] Value in parentheses indicate number of monomers in 1-start helix

[3] The average value is taken from Fig. 3J, and the median diameter is shown in parentheses

[4] The pitch of the constricted helix varies, but it does not decrease (i.e. no compression)

[5] The predicted # of subunits per turn is based on the average measured circumference and the assumption that the helical path length does not change

[6] Value based on the predicted # of subunits per turn